Delft University of Technology

AE3211-I

Meeting the goal of sustainability in the regional transport: the ATR 72-HE

Group 57

Anton Hendrickx	4803671
Aderik Verraest	5234190
Szymon Błazucki	5345758
Jan Kulik	5327377
Dragomir Nikolov	5216915
Mike Timmerman	5216796

Figure 0.1: ATR 72-600 (credits @ATR)

March 12, 2025

Contents

1: Assessment of the reference aircraft

In the following chapter the current version of the ATR72, the ATR72-600, will be analyzed in terms of weight and balance. In section 1.1 the sources used to obtain several aircraft parameters are discussed. In section 1.2 the main weight contributions of the aircraft are shown. In section 1.3 the center of gravity of all aircraft components are calculated and discussed. In section 1.4 the loading diagram along with its assumptions is presented and discussed. In section 1.5 the stability and control of the aircraft is discussed by obtaining a scissor plot.

1.1 Familiarization

In order to familiarize with the aircraft, several sources were consulted. First of all, the World's Aircraft Catalogue, Janes [1] was consulted to obtain several main parameters of the ATR72-600. Besides, the official ATR website [2] was consulted to obtain the cabin layout for a seat pitch of 29 inch, as shown in Figure 1.1. To obtain detailed measurements of the aircraft's geometry, engineering drawings were obtained from [3]. The detailed engineering drawings can be found in Appendix B. The relevant parameters obtained from each of these sources will be mentioned throughout the document with their respective source.

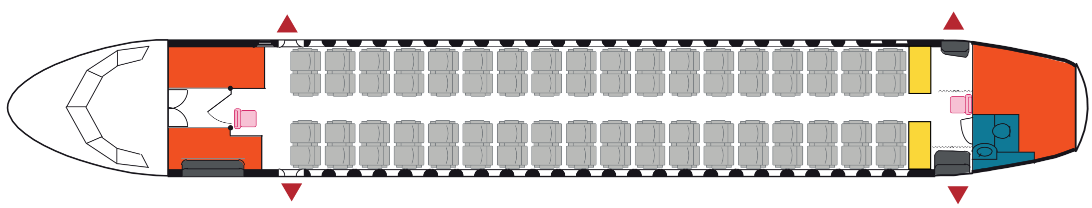

Figure 1.1: Cabin layout of ATR72-600 with 29 inch seat pitch. Image taken from [2]

1.2 Weight contributions

An aircraft has three main weight contributions: the operational empty weight (OEW), fuel and payload. These weight contributions are summarized along with the maximum take off weight (MTOW) in Table 1.1 and Figure 1.2.

Table 1.1: Weight contributions of the ATR72-600, obtained from [1]

Weight contribution	Weight [kg]	Weight [% MTOW]
MTOW	22800	100
OEW	13315	58.4
Max payload	7500	32.9
Max fuel	5000	21.9

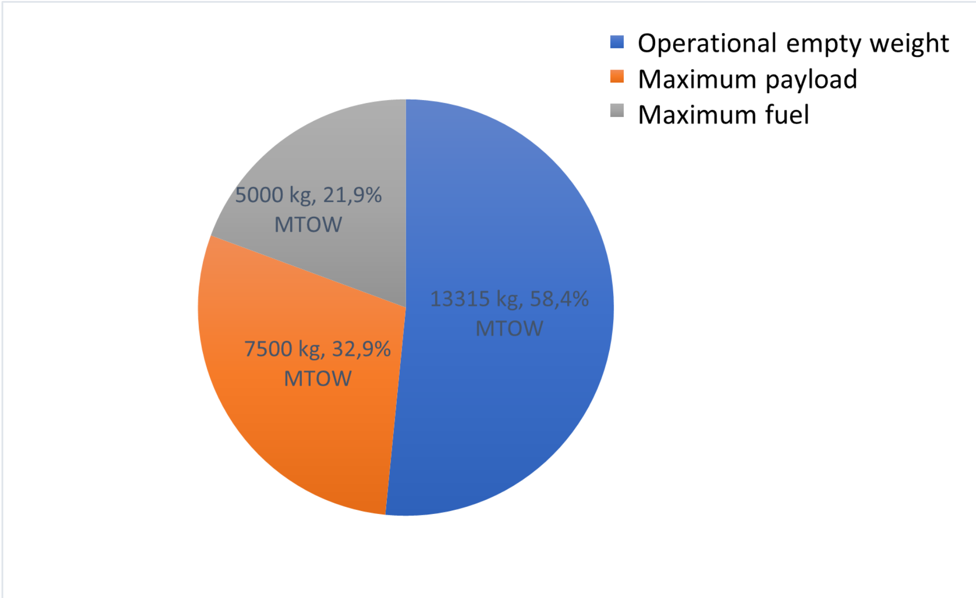

Figure 1.2: Weight pie chart

1.3 CG locations

In order to accurately determine the weight and balance of the aircraft, first the CG locations of all individual components must be used. For the wing, horizontal tail, vertical tail and fuselage they were determined using the Class II CG location estimation method in Figure 1.3. For both landing gears the center of gravity is assumed to be at the centroid of the wheels. For the propulsion system, the center of gravity was determined using informed engineering judgement. All measurements were done using the engineering drawings giving in Appendix B. The weights of all individual components were given as a percentage of the MTOW in [4] and are given in Table 1.2. The results of the CG location estimation calculations and measurements can be found in Table 1.3.

To calculate the fuel center of gravity, the front and back position of the fuel tank w.r.t. the root chord were obtained from [5]. Likewise, the centroid of the root airfoil between $0.12 \cdot c_{root}$ and $0.85 \cdot c_{root}$ can be calculated and is assumed to be the stationary center of gravity location of the fuel.

The datum point in front of the aircraft is obtained from the Figure B.1, and is determined to be $2362mm$ in front of the nose aircraft. The MAC is $2303mm$ and the $LEMAC$ is $13604mm$ to the back of the datum point of the aircraft, which are obtained from [6].

Part V Chapter 8 Page 114

Table 8.1 Center of Gravity Location of Structural Components

Component:	Center of gravity location:
Wing (half):	Unswept wing: 38-42 percent chord from the L.E. at 40 percent of the semi-span. Swept wing: 70 percent of the distance between the front and rear spar behind the front spar at 35 percent of the semi-span
Horizontal Tail: (half)	Regardless of sweep angle: 42 percent chord from the L.E. at 38 percent of the semi-span.
Vertical Tail: (low tail)	Regardless of sweep angle: 42 percent chord from the L.E. at 38 percent vertical tail span from the root chord.
Vertical Tail: (T-tail) root	Regardless of sweep angle: 42 percent chord from the L.E. at 55 percent vertical tail span from the root chord.
Vertical Tail: (cruciform)	Regardless of sweep angle: 42 percent chord from the L.E. at between 38 and 55 percent vertical tail span from the root chord. Interpolate according to z_h/b_v.
Fuselage: Caution: Do not count the propeller spinner in fuselage or nacelle length!	Distances are given as a fraction of the fuselage length: Single engine tractors: 0.32-0.35 Single engine pusher: 0.45-0.48 Propeller driven twins: 0.38-0.40 (tractors on wing) Propeller driven twins: 0.50-0.53 (pushers on wing) Jet transports: 0.42-0.45 (wing mounted engines) Jet transports: 0.47-0.50 (rear fuselage mounted engines) Fighters: 0.45 (engines buried in the fuselage)
Tail booms:	0.40-0.45 of boom length starting from most forward structural attachment of the boom.
Nacelles:	0.40 of nacelle length from nacelle nose
Landing gear:	at 0.50 of strutlength for gears with mostly vertical struts

Figure 1.3: Class II CG location estimation method. Image taken from Roskam [7].

Table 1.2: Weight breakdown. Table taken from [4].

Component	Weight [% MTOW]
Wing	14.9
Horizontal Tail	1.8
Vertical Tail	2.0
Fuselage (including cabin and cockpit systems)	24.8
Main Landing Gear	3.5
Nose Landing Gear	0.5
Propulsion (including nacelle)	10.3

Table 1.3: Weights and CG locations of the ATR72-600 components and groups.

	Group	Component	Weight [% MTOW]	Weight [kg]	CG location w.r.t front datum [m]	CG location w.r.t LEMAC [m]	CG location w.r.t LEMAC [MAC]
OEW	Fuselage	Horizontal tail	1.8%	410	27.86	14.26	619.0%
	Fuselage	Vertical tail	2.0%	456	26.69	13.08	568.0%
	Fuselage	Fuselage	24.8%	5654	12.65	-0.95	-41.3%
	Fuselage	Nose Gear	0.5%	114	4.09	-9.52	-413.3%
	Wing	Wing	1.49%	3397	14.20	0.59	25.7%
	Wing	Main gear	3.5%	798	14.87	1.26	54.8%
	Wing	Propulsion	10.3%	2348	12.44	-1.17	-50.6%
		Other	0.6%	137			
		Fuselage group	29.1%	6635	14.41	0.81	35.0%
		Wing group	28.7%	6544	13.65	0.04	1.8%
		Total	58.4%	13315	14.03	0.43	18.5%
Max payload		Total	32.9%	7500			
Max fuel		Total	21.9%	5000	14.79	1.18	51.4%

1.4 Aircraft loading diagram

In order to obtain the aircraft loading diagram, first the center of gravity of each luggage compartment and each row must be determined. This can be done by measuring them on the engineering drawings. The measured parameters can be found in Table 1.4. For the cargo compartments, the CG is assumed to be the average of the front and back wall of the respective compartment. To determine the CG of the consequent rows after the first row, linear extrapolation is used using the seat pitch of 29$inch$. The weights for each individual payload can be found in Table 1.5. To determine the loading diagram, extreme cases have to be considered to be able to prevent the aircraft from tipping over or to prevent too much weight being placed on the front landing gear resulting in less effective breaking power. For the ATR 72-600, the loading procedure is as follows, first the cargo is loaded, then the passengers following the window aisle method [4], meaning first the passengers at the windows board and after the passengers who are sat at the aisle. Lastly the aircraft is fueled [4]. The most extreme cases in this process occur when the loads that are added, being cargo/passengers/fuel are not distributed properly. In other words, the cargo would first be loaded completely in the front cargo department before starting to place cargo in the aft department or the other way around. Similarly for the passengers, by filling up the aircraft from front to back or back to front. Considering these 2 loading extremes result in the 'potato shapes' that can be seen on Figure 1.5. The C.G limitation (black dotted line) was calculated with 2% margins from the actual extreme values to account for personnel or passengers moving or other small occurrences that might have an influence on the center of gravity.

Table 1.4: CG locations for the payload components

Number on Figure 1.4	Location	Distance w.r.t. nose [m]	Distance w.r.t. datum [m]	Distance w.r.t. LEMAC [m]	Distance w.r.t. LEMAC [MAC]
1	front wall cargo front	3.38	5.71	-7.90	-3.43
2	front wall cargo back	5.41	7.74	-5.87	-2.55
	estimated CG cargo front	4.40	6.72	-6.88	-2.99
3	first row	5.96	8.29	-5.32	-2.31
4	front wall cargo back	20.32	22.64	9.04	3.92
5	back wall cargo back	22.48	24.81	11.20	4.86
	estimated CG cargo back	21.40	23.72	10.12	4.39

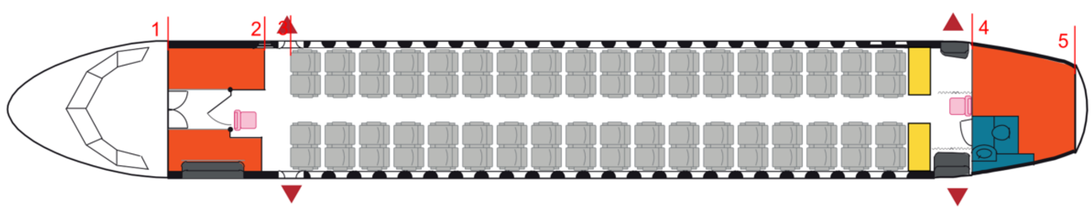

Figure 1.4: CG locations in the ATR72-600 aircraft cabin. Numbers overlay own work. Background image taken from [2].

Since the fuel tank is located fairly close to the mean aerodynamic center, the c.g. limitations will never be dependent of the amount of fuel [1.6], since it will not result in large moments around the MAC. Therefore the choice was made to inspect the extreme loading cases under maximum payload conditions. Since the ATR 72-600 has a maximum payload of 7500kg [1] and a weight per passenger was assumed to be 80kg, the additional cargo that could be added was 1740kg (approximately 24kg per passenger, but of course it could be a flight transporting both cargo and passengers). This will be done by dividing the cargo equally over the front and aft cargo compartment as described before. The fuel that can be added after all this is equal to the (MTOW - OEW - payload) resulting in a fuel load of 1984.8kg. The values are summarized in Table 1.5.

Table 1.5: Weights for payload

	Weight [kg]
Cargo per bay	870
Fuel on board	1984.8
Weight per passenger	80

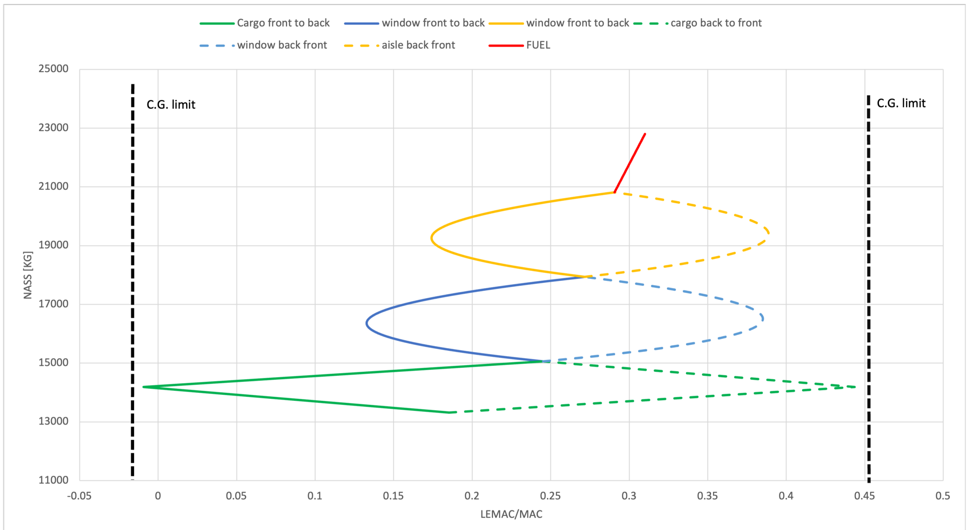

Figure 1.5: Loading diagram of ATR72-600

As can be seen in Figure 1.5, the c.g. limits are clearly dependent on the cargo being added, this makes sense since the cargo compartments are located at a relatively far distance from the MAC and this in combination with the relatively high weights added result in high moments. It can also be observed that fuel indeed has a low impact on the c.g. limitations as a very large quantity would have to be added in order to become the limiting factor, far more than the maximum fuel load allows [1]. The numerical values are of these extremes are provided in Table 1.6. Note that the ranges of the c.g. always represent the following case [front to back, back to front].

Attribute	**c.g. [MAC]**
OEW	18.53%
front cargo compartment	−299%
rear cargo compartment	439%
fuel tank	51.4%
c.g. range during operation	**c.g.[MAC]% [min, max]**
cargo loading window passengers loading aisle passengers loading fuel loading	[−0.9332, 45.23] [13.27, 38.513] [17.41, 38.875] [29.062, 31.007]
Extreme loading case	**c.g. [MAC], including margin**
[**MAX**] loading cargo back to front	45.23%
[**MIN**] loading cargo front to back	−0.915%

Table 1.6: Extreme loading cases

1.5 Scissor plot

Scissor plots provide a visualization of the aircraft's controllability and stability as a function of its center of gravity and horizontal tail area ratio S_h/S. The scissor plot for the ATR72-600 we obtained can be found in Figure 1.6. Everything to the top-right of the green 'Control' line is controllable. Everything to the top-left of the 'Stability with/without margin' line is stable. The entire CG range should fall within this range in order to have a controllable and stable aircraft. In the following Table 1.7 the geometric parameters used to obtain these plots are given. The majority of these parameters have been measured on the engineering drawings given in Appendix B. Other parameters were obtained from [1].

Table 1.7: Geometric parameters used

variable	note	value	unit	variable	note	value	unit
l_f	fuselage length	27.165	[m]	λ_h	horizontal tail taper ratio	0.642	[−]
h_f	fuselage height	2.635	[m]	A_h	Aspect ratio horizontal tail	4.61	[−]
b_f	fuselage width	2.865	[m]	c_r	wing root chord	2.57	[m]
b	wing span	27.05	[m]	c_t	wing tip chord	1.59	[m]
$\bar{c}$	MAC	2.303	[m]	S_h	horizontal tail surface area	11.57	$[\mathrm{m}^2]$
S	wing area	61	$[\mathrm{m}^2]$	b_h	horizontal tail span	7.310	[m]
λ	taper ratio	0.619	[−]	X_{MAC}	mean aerodynamic chord location	13.604	[m]
$\Lambda_{0.25}$	wing sweep 1/4c	1.5	[deg]	V_h/V	speed downwash effect	0.95	[−]
$\Lambda_{0.50}$	wing sweep 1/2c	2.5	[deg]	l_h	horizontal tail arm	14.08	[m]
$\Lambda_{h_{0.5}}$	horizontal tail sweep 1/2c	1.3	[deg]	A_w	aspect ratio wing	12	[−]

1.5.1 Stability equation

The stability curve is represented by Equation 1.1, in order to use this formula, more variables have to be calculated. The formulas to find these variables and parameters will be used as described in the lecture slides from the course [8].

$$\frac{S_h}{S} = \frac{1}{\left[\frac{C_{L\alpha_h}}{C_{L\alpha_{A-h}}}\left(1-\frac{d\varepsilon}{d\alpha}\right)\frac{l_h}{\bar{c}}\left(\frac{V_h}{V}\right)^2\right]} x_{cg} - \frac{\bar{x}_{ac}-0.05}{\frac{C_{L\alpha_h}}{C_{L\alpha_{A-h}}}\left(1-\frac{d\varepsilon}{d\alpha}\right)\frac{l_h}{\bar{c}}\left(\frac{V_h}{V}\right)^2} \tag{1.1}$$

1.5.2 Control equations

The control curve is represented by Equation 1.2, again, in order to use this formula, many more variables have to be calculated. Also here will the lecture slides be used to do so. [8].

$$\frac{S_h}{S} = \frac{1}{\frac{C_{L_h}}{C_{L_{A-h}}}\frac{l_h}{\bar{c}}\left(\frac{V_h}{V}\right)^2} \cdot x_{cg} + \frac{\frac{C_{m_{ac}}}{C_{L_{A-h}}} - \bar{x}_{ac}}{\frac{C_{L_h}}{C_{L_{A-h}}}\frac{l_h}{\bar{c}}\left(\frac{V_h}{V}\right)^2} \tag{1.2}$$

1.5.3 Plot

The obtained scissor plot for the ATR72-600 is given in Figure 1.6. The parameters used to obtain this scissor plot can be found in Table 2.4. It is clear that the aircraft is both controllable (although by a very small margin) and stable (by a more comfortable margin), which makes sense, since it is a certified aircraft.

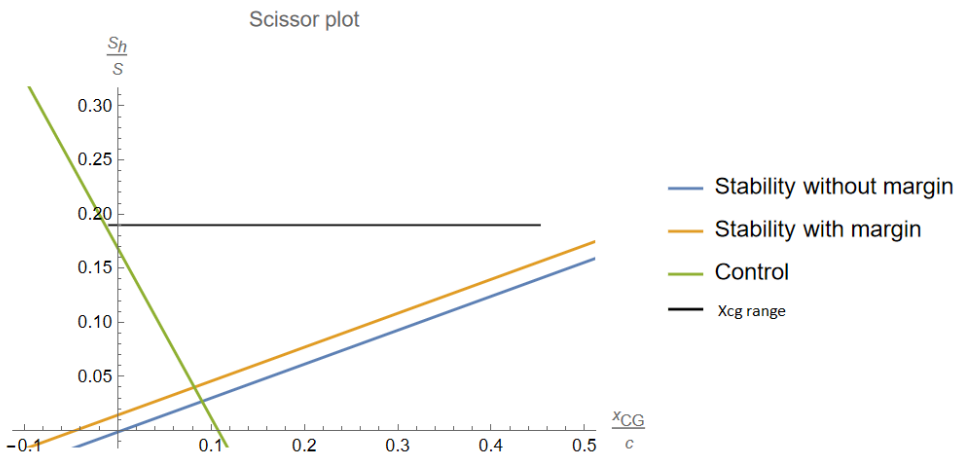

Figure 1.6: Scissor plot for the ATR72-600

2: Evaluation of design modifications

The RD department of ATR has come up with several design modifications for the ATR72-HE, which will be described below (the list has been cited from [4]):

- The effective aspect ratio is 20% higher than the geometric AR thanks to innovative winglets;
- The nacelles have increased dimensions in both diameter (+25%) and length (+15%) in order to accommodate other subsystem and allow a proper cooling condition of the components;
- The overall weight of the propulsion system hasn't varied with respect the conventional version; on the other side, the weight of the wing group is 10% lighter than the initial one and the fuselage weight results increased by 2% (always when compared to the initial value);
- The last two rows of passenger are removed;
- The electric part of the powertrain is powered by two battery packs. The first pack is located just underneath the CG of the front cargo area and it weighs 400 kg. The second battery pack is located underneath the rear cargo area and it weighs 800 kg. The battery are not removable and it is explicitly noted that a new CG@EOW+Batt shall be calculated;
- The MTOW of the aircraft will be kept constant by assuming that a modification of the amount of embarked fuel will compensate any weights difference [4]

In section 2.1 the effects of the design modifications on weight and balance are discussed. In section 2.2 the effects on the aircraft loading diagram are shown and discussed. In section 2.3 the update control and stability requirements, and whether they are satisfied, are discussed. In section 2.4 the feasibility study is concluded by answering several customer questions.

2.1 Effect on weight & balance

The design changes that affect the weight and balance of the aircraft have been incorporated in Table 2.1. The changes w.r.t. the ATR72-600 are indicated in green. For comparison of the values of the ATR72-HE with the ATR72-600, Table 1.3 can be consulted. It is most noticeable that the decrease in the weight of the wing group is not able to compensate the increase due to the batteries, resulting in an OEW that is about 659kg higher, reducing the fuel one can take for max payload or vice-versa for the ATR72-HE compared to the ATR72-600. The new main weight contributions are summarized in Table 2.2 and Figure 2.1.

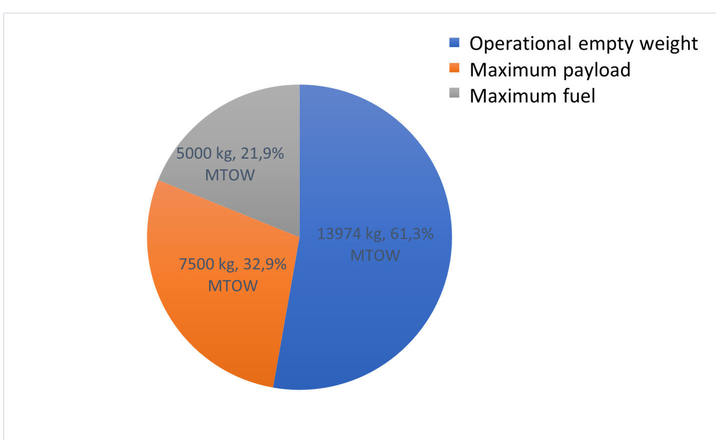

Figure 2.1: Weight pie chart

Table 2.1: Weights and CG locations of the ATR72-HE components and groups. The differences with the ATR72-600 are indicated in green.

	Group	Subcomponent	Weight [% MTOW]	Weight [kg]	cg location w.r.t front [m]	cg location w.r.t LEMAC [m]	cg location w.r.t LEMAC [MAC]
OEW	Fuselage	Horizontal tail	1.8%	410	27.86	14.26	619.0%
	Fuselage	Vertical tail	2.0%	456	26.69	13.08	568.0%
	Fuselage	Fuselage	25.3%	5767	12.65	-0.95	-41.3%
	Fuselage	Nose Gear	0.5%	114	4.09	-9.52	-413.3%
	Fuselage	Front batteries	1.8%	400	6.72	-6.88	-298.9%
	Fuselage	Back batteries	3.5%	800	21.40	7.79	338.4%
	Wing	Wing	14.9%	3397	14.20	0.59	25.7%
	Wing	Main gear	3.5%	798	14.87	1.26	54.8%
	Wing	Propulsion	10.3%	2348	12.60	-1.01	-43.8%
		Other	0.6%	137			
		Fuselage group	34.9%	7948	14.70	1.10	47.7%
		Wing group	25.8%	5889	13.70	0.10	4.3%
		total	61.3%	13974	14.28	0.67	29.2%
Max payload		total	32.9%	7500			
Max fuel		total	21.9%	5000	14.79	1.18	51.4%

Table 2.2: Weight contributions of the ATR72-HE. Apart from the OEW obtained from [1]

Weight contribution	Weight [kg]	Weight [% MTOW]
MTOW	22800	100
OEW (+ batteries)	13974 (+659)	61.3 (+2.9)
Max payload	7500	32.9
Max fuel	5000	21.9

.

2.2 Effect on loading diagram

The loading diagram for the ATR72-HE is given in Figure 2.2. It is clear that the CG range became smaller, except for the cargo, and that the CG range shifted backwards. This is due to the lower number of passengers, allowing more cargo to be taken for the same maximum payload. Moreover, the OEW shifted slightly backward (influencing the CG position) and became heavier (making the relative CG range smaller compared to the ATR72-600, except for the cargo).

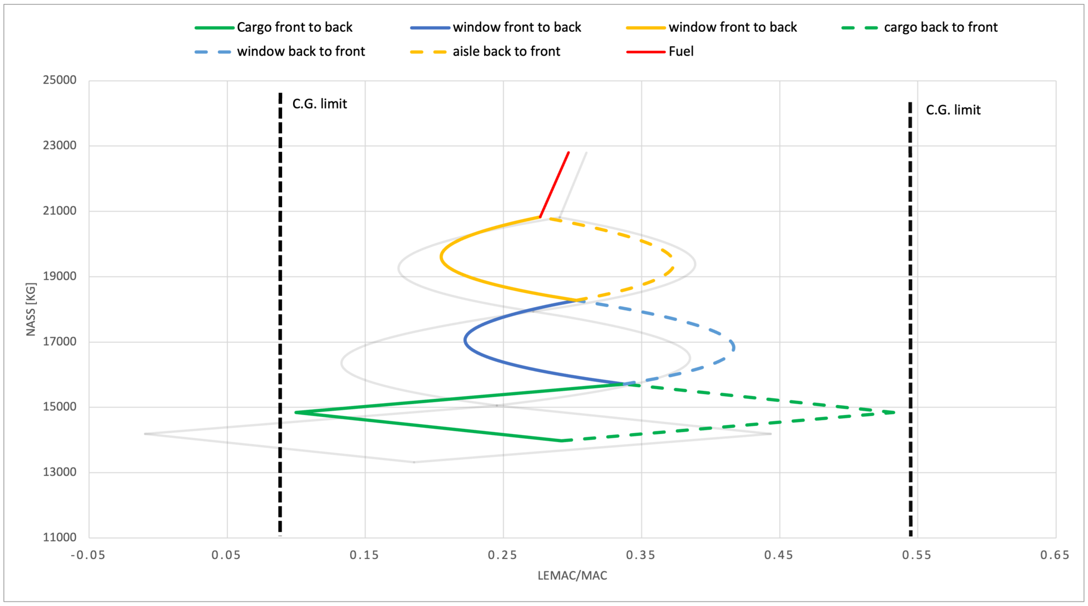

Figure 2.2: Updated loading diagram, grey being the previous diagram

Attribute	**c.g. [MAC]**
OEW	29.201%
front cargo compartment	−299%
rear cargo compartment	439%
fuel tank	51.4%
Extreme loading case	**c.g. [MAC], including margin**
[**MAX**] loading cargo back to front	54.309%
[**MIN**] loading cargo front to back	9.776%

Table 2.3: Extreme loading cases for ATR 72-HE

2.3 Effects on control & stability

The scissor plot for the ATR72-HE can be seen in Figure 2.3. The parameters used to obtain this scissor plot can be found in Table 2.4. It is noticeable that the aircraft has a much larger margin for controllability than the ATR72-600, which makes sense, since the OEW is moved slightly back and is slightly heavier, increasing its contributions to the moment. The stability with margin however, is not satisfied by a small amount. Solutions for this will be discussed in section 2.4.

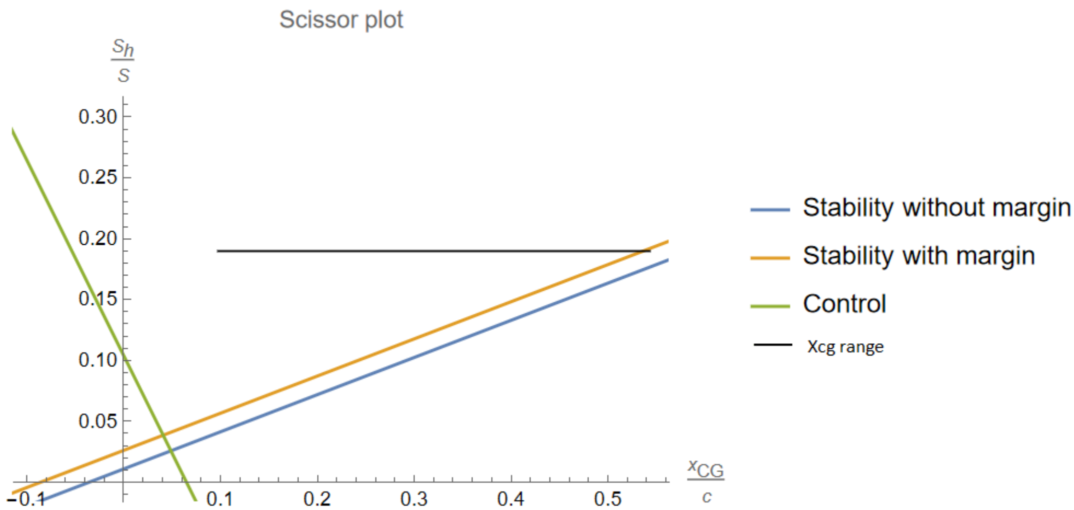

Figure 2.3: Scissor plot for the ATR72-HE

Paramter	ATR 72-600	ATR 72-HE
Cruise speed	509 $\frac{km}{h}$	509 $\frac{km}{h}$
Approach speed	185.2 $\frac{km}{h}$	185.2 $\frac{km}{h}$
$\frac{V_h}{V}$	0.95	0.95
$C_{L_{\alpha_h}}$	4.22006	4.22006
$C_{L_{\alpha_{A-h}}}$ wing contr. fusalage contr.	5.93059 5.48976 0.440831	6.09582 5.64839 0.447426
$\frac{d\eta}{d\alpha}$	0.228406	0.195838
$\bar{x}_{ac}$ at V_{cruise} $\bar{x}_{ac_{wing}}$ at V_{cr} $\bar{x}_{ac_{fus}}$ at V_{cr} $\bar{x}_{ac_{nac}}$ at V_{cr}	0.00505363 0.24 -0.213169 -0.021777	-0.00528462 0.24 -0.207214 -0.0380711
$\bar{x}_{ac}$ at V_{ap} $\bar{x}_{ac_{wing}}$ at V_{ap} $\bar{x}_{ac_{fus}}$ at V_{ap} $\bar{x}_{ac_{nac}}$ at V_{ap}	−0.022 0.24 −0.238 −0.0243	−0.035 0.24 −0.232 −0.043
$(C_{L_h})_{max}$ for fixed tail	-1.0301	-1.0301
$C_{m_{ac}}$ $C_{m_{ac_{wing}}}$ $\Delta_{fl} C_{m_{ac}}$ $\Delta_{fus} C_{m_{ac}}$ $\Delta_{nac} C_{m_{ac}}$	-0.3744 −0.0171116 −0.29 −0.0573763 -	-0.373549 −0.0175287 −0.29 −0.0560204 -

Table 2.4: Relevant stability and control parameters for the ATR72-600 and ATR72-HE.

2.4 Costumer questions

In the following section the feasibility study will be concluded by answering several customer questions:

- How do the aforementioned design modifications affect both longitudinal stability and controllability?

  The modifications allow to shift x_{cg} forward much further - even though the most forward cg position shifted more backward - but slightly violates the stability margin.

- Would it be still possible to fulfill the longitudinal SC requirements without changing the current horizontal tail size, longitudinal wing position and stability margin?

  Because the stability margin violation is not that severe, the stability margin can be easily satisfied by manipulating the cg-range. Some possible changes the would shift the cg-range more forward would include, but are not limited to:

  - Putting more battery weight in the front of the aircraft and less in the back of the aircraft.
  - Slightly reducing the maximum payload, such that there is less cargo allowed and thus the cargo influences the center of gravity less (see also Figure 2.2).
  - Allowing more passengers, such that there is less cargo and thus the cargo influences the center of gravity less (see also Figure 2.2).

- How smaller could be the horizontal tail size, while still fulfilling both the longitudinal SC constraints and without modifying the longitudinal position of the wing neither the stability margin?

  The horizontal tail cannot become smaller, since the stability margin would scarcely be satisfied.

- In this case what would become the critical longitudinal requirement? Stability or control?

  Although in the original design controllability was the critical requirement, in the new version stability is the critical requirement.

- What design iterations (if any) would be necessary to confirm your answer? (provide just a qualitative answer)

  Try the changes previously described to move the CG range (like moving batteries, reducing max payload, increasing number of passengers...).

- Is there any modification on the longitudinal position of the main landing gear that is needed to guarantee stability during the take-off maneuver?

  The main landing gear is more than sufficiently positioned to the back of the aircraft (126% MAC Table 1.3) to guarantee stability during the take-off manoeuvre.

- Would you suggest a different combination of rear and front battery pack in order to improve stability and controllability characteristics.

  Yes, as described previously, ideally more battery weight would be in the front of the aircraft and less in the back.

Bibliography

[1] *Atr72-600*, Jun. 2022. [Online]. Available: https://customer.janes.com/explorer/Equipment_8629?selectedNode=specifications&explorerState=f5e763f9-18a8-496c-8b65-b1b6d00840dd.

[2] ATR Aircraft, *ATR 72-600*, https://www.atr-aircraft.com/our-aircraft/atr-72-600/, n.d.

[3] *ATR 72-600*, http://www.airwar.ru/enc/aliner/atr72-600.html, Accessed on April 5, 2023, n.d.

[4] Student name, *Meeting the goal of sustainability in the regional transport: the ATR 72-HE*, Assignment in light of Systems Engineering and Aerospace Design (AE3211-I) 2022/2023-Regular Session course, 2023.

[5] All Time Reset, *ATR 72-600 Fuel System*, https://alltimereset.weebly.com/fuel.html, n.d.

[6] A. Carlo, *Wbm atr 72*, Apr. 2021. [Online]. Available: https://www.scribd.com/document/502449710/WBM-ATR-72.

[7] J. Roskam, *Airplane Design* (Airplane Design dl. 5). DARcorporation, 1985, ISBN: 9781884885501. [Online]. Available: https://books.google.be/books?id=mMU47Ld7yQkC.

[8] F. Oliviero, *Systems engineering & aerospace design*, Course code AE3211-I taught at Delft University of Technology, 2023.

A: Task Distribution

In order for this assignment to be executed in a proper, organized manor, team roles where determined before the project started such that there was a clear overview. Each member had their own role and their associated duties. Because of the nature of the project (having 2 parts) it was decided to assign one overall leader, who would keep a clear overview of both assignments and deliverables that needed to be done, and 2 assignment coordinators who would focus more in detail on a specific part such that a high standard of reporting and execution was assured. The exact organization of the team can be seen in Figure A.1.

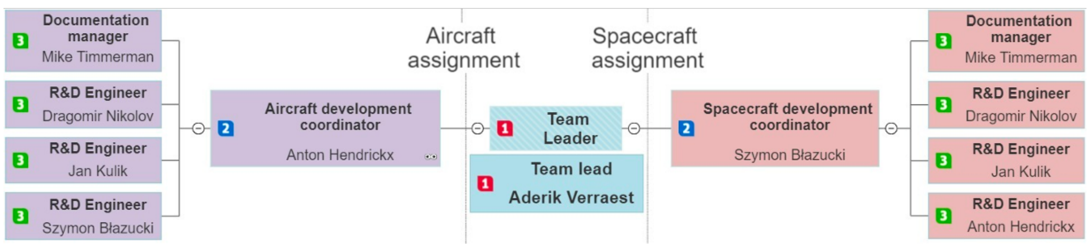

Figure A.1: Team distribution during the project

A more in debt overview of which team member worked on what part is included in Table A.1

section	name
familiarization	all
weight contributions	Aderik, Drago
CG locations	Aderik, Jan
Aircraft loading diagram	Anton, Mike
Scissor plot	Anton, Szymon, Mike
Effect on weight and balance	Aderik, Drago
Effects on loading diagram	Anton, Mike, Szymon
Effects on control and stability	Anton, Szymon, Drago
Costumer questions	Aderik, Drago, Jan
task distribution	Anton, Jan

Table A.1: Task distribution per section

B: Engineering Drawings

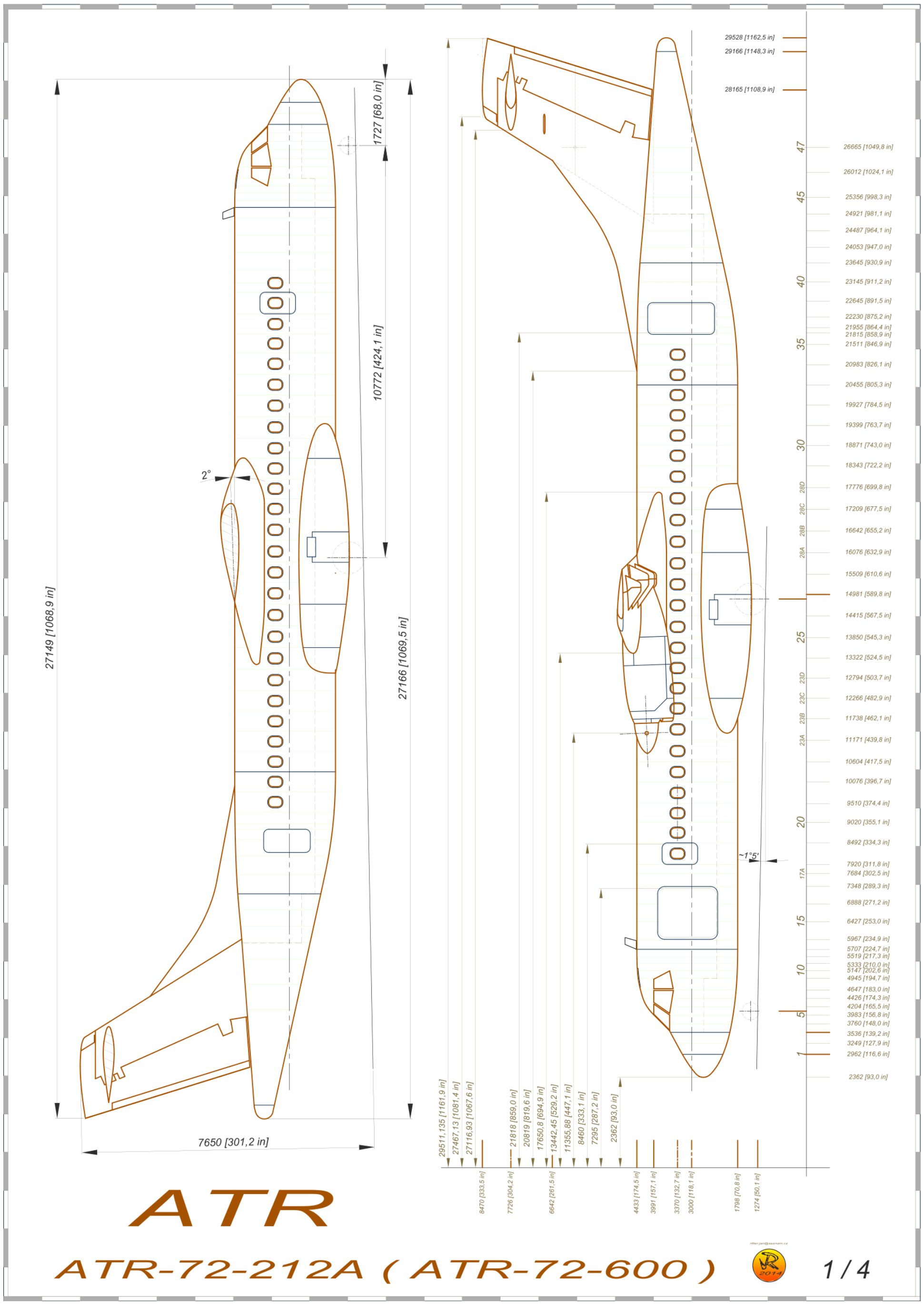

Figure B.1: Side view engineering drawing of ATR72-600. Image taken from [3].

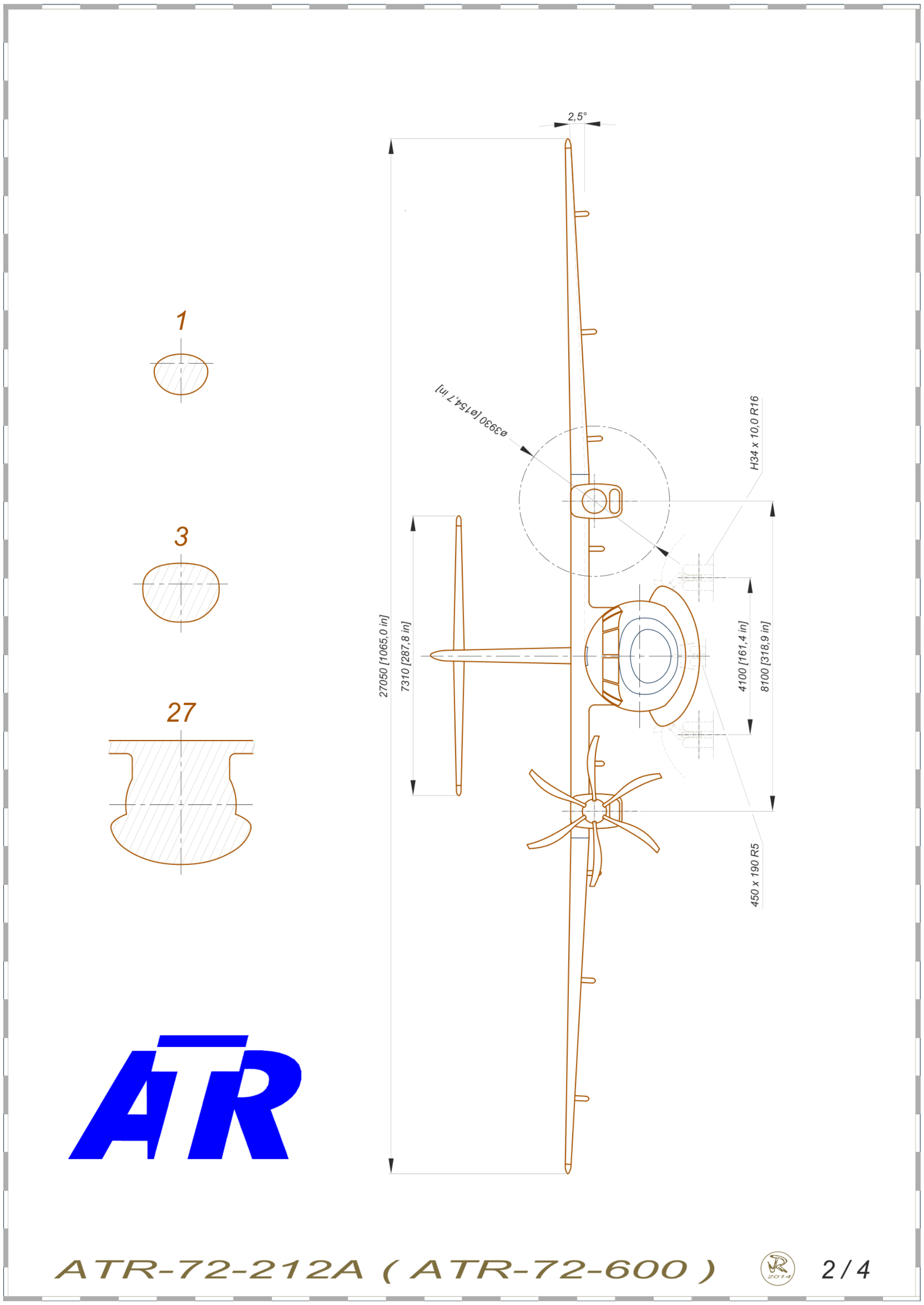

Figure B.2: Front view engineering drawing of ATR72-600. Image taken from [3].

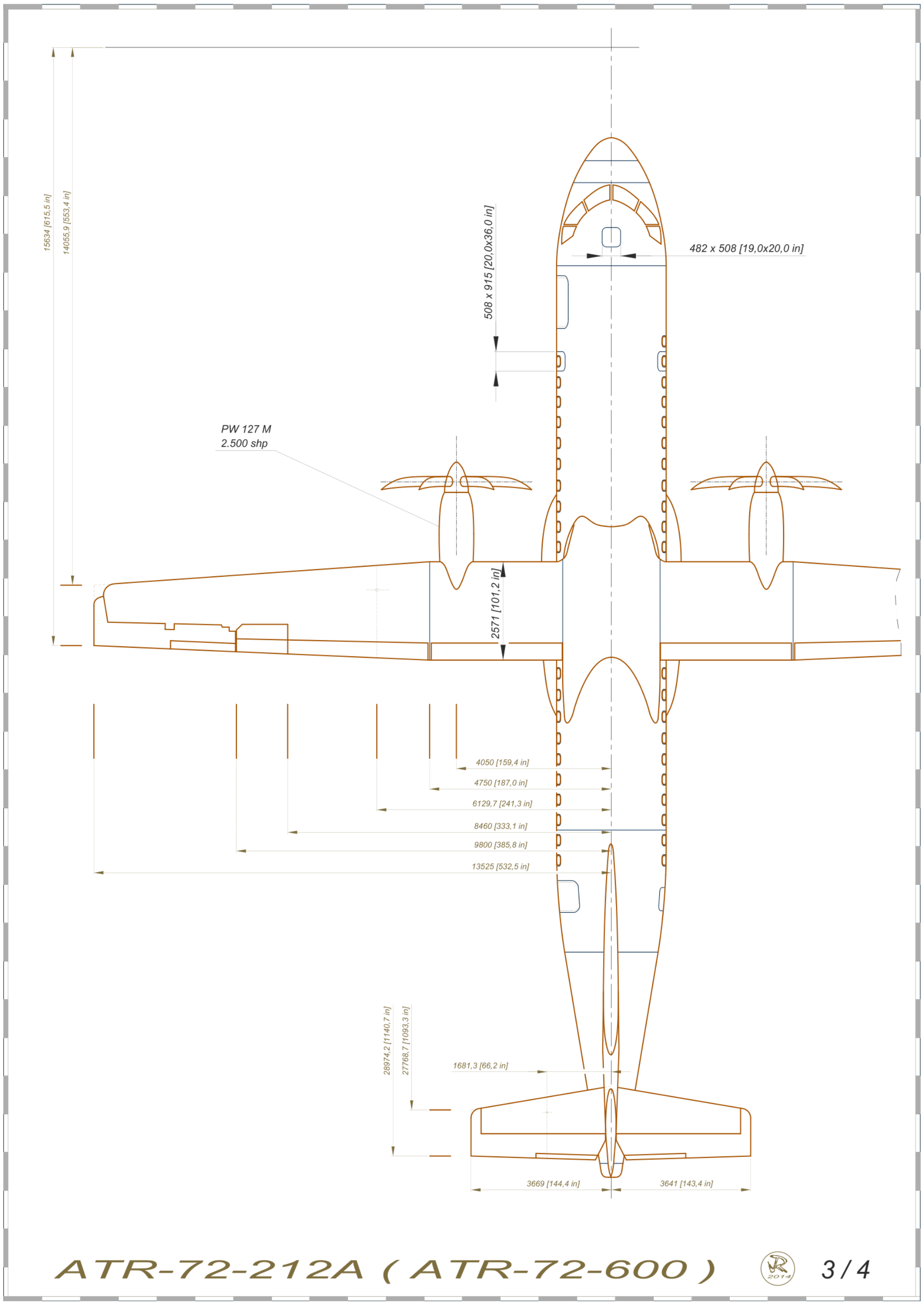

Figure B.3: Top view engineering drawing of ATR72-600. Image taken from [3].

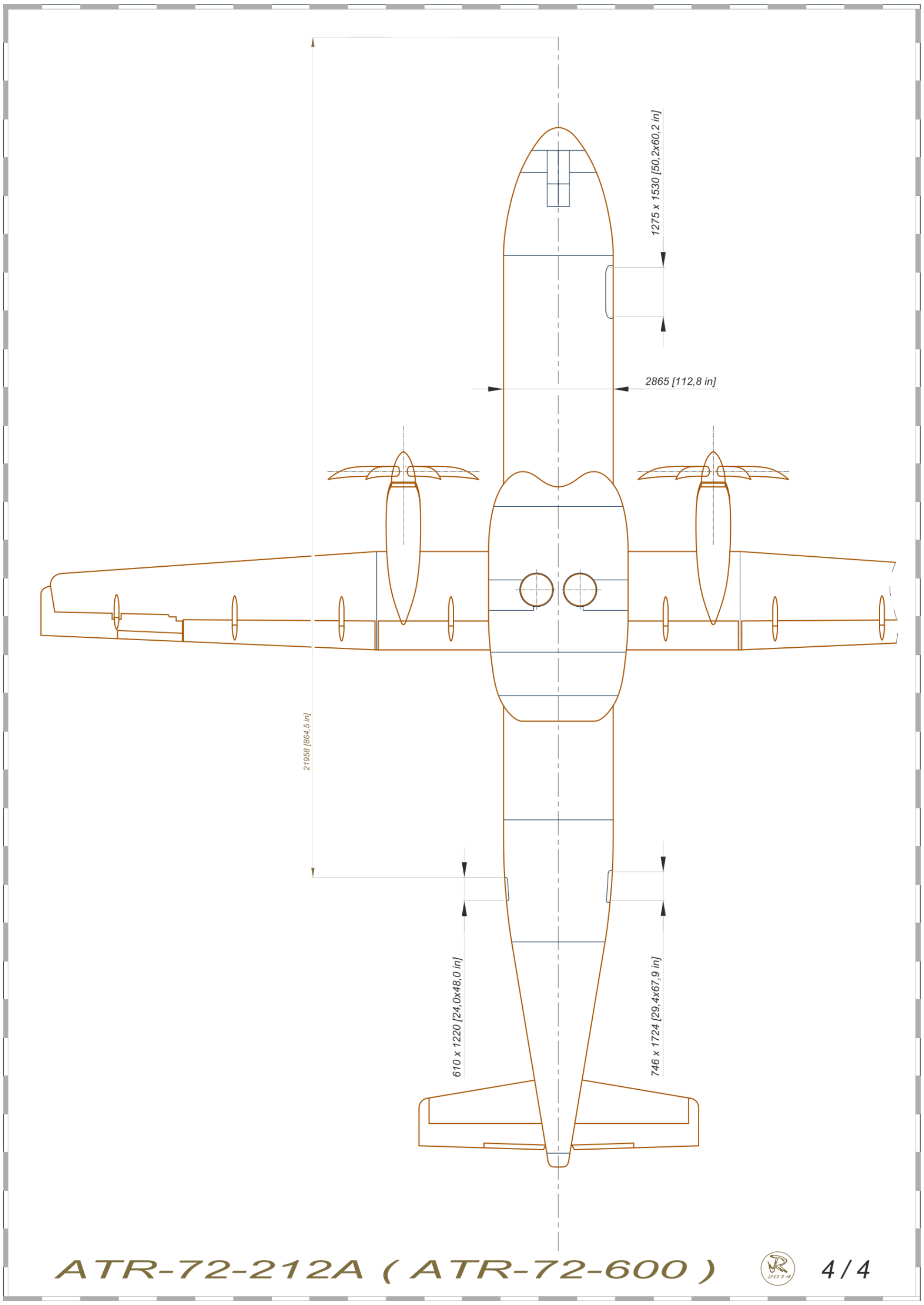

Figure B.4: Bottom view engineering drawing of ATR72-600. Image taken from [3].